Inorg. Chem. **2007**, *46*, 8812–8818

Syntheses and Structures of New Phases AeM_xIn_{4-x} (Ae = Sr, Ba; M = Mg, Zn): Size Effects and Site Preferences in $BaAl_4$-Type Structures

Bin Li and John D. Corbett*

Ames Laboratory, U.S. DOE and Department of Chemistry, Iowa State University, Ames, Iowa 50011

Received June 8, 2007

The title phases were synthesized via high-temperature solid-state methods and structurally characterized by single-crystal X-ray diffraction. The phase widths of both $SrMg_xIn_{4-x}$ ($0.85 \le x \le 1.53$) and $BaMg_xIn_{4-x}$ ($0 \le x \le 1.79$) are consistent with size matches between Ae and the encapsulating M–In cages. All compounds crystallize in body-centered tetragonal $BaAl_4$-type structure (*I*4/*mmm*, $Z = 2$) except that $SrMg_xIn_{4-x}$, $0.85 \le x \le 1.24$, occurs in the lower-symmetry space group ($I\bar{4}m2$, $Z = 2$) and the atoms are all ordered at the composition $SrMgIn_3$. The substitution of the effectively smaller Mg or Zn atoms into the indium sublattice of the monoclinic $SrIn_4$ (*C*2/*m*) dramatically changes the structure into the tetragonal $BaAl_4$-type structure. Compared with the Mg compounds in which all Mg occupy the basal 4d crystallographic site, Zn occupies the other 4e (apical) site in both $BaZn_{0.79(2)}In_{3.21}$ and $SrZn_{1.00(4)}In_{3.00}$. These differences are related to the interplay of size and electronic factors. The latter may be expressed by not only electronegativities but also total energies according to linear muffin-tin-orbital calculations.

Introduction

Polar intermetallic compounds represent a link between charge-balanced Zintl phases and fully delocalized metallic systems. This situation is especially evident in systems of alkali or alkaline-earth metals with post-transition metals. The p elements are formally reduced by the electropositive component and form polyanionic clusters or networks.[1] However, compared with classical Zintl phases, the structures of polar intermetallics are not easily rationalized since electron localization and closed-shell bonding rules lose their importance, and factors beyond covalent bonding effects become competitive in structure selection, namely, the mutual optimization of the Madelung (site) energies and size and packing effects. Such complex situations have been illustrated through extensive studies on the structures of $SrIn_4$[2] and on a variety of ternary $BaAl_4$-family compounds.[3] The large majority of 1:4 alkaline-earth-metal−triel compounds realize the simple tetragonal $BaAl_4$ structure type, whereas the $SrIn_4$ compound crystallizes in the rarely adopted and totally different monoclinic structure type mainly because of the atomic size mismatching.

The $BaAl_4$-type structure is widely adopted among AeE_4 intermetallic compounds that are often of interest because of their electronic and bonding characteristics.[3,4] The structure features a body-centered tetragonal unit cell (space group *I*4/*mmm*, No. 139) (Figure 1a). There are two independent E sites: the basal atoms (E_b) occupy Wyckoff 4d sites ($0,{}^1/_2,{}^1/_4$) and form two-dimensional square nets which are alternately capped above and below the plane by the apical atoms (E_a) in Wyckoff 4e sites (0,0,*z*). The Ae atom sits in the center of an 18-vertex Fedorov polyhedron[5] defined by 8 E_b atoms and 10 E_a atoms (Figure 1b). The cube defined by the eight atoms of the latter generally exhibits the shortest distances to Ae. The binary examples of pertinence here are $AeAl_4$ and $AeGa_4$, which exist for Ae = Sr, Eu, and Ba[6] and for $BaIn_4$.[7] This well-known structure is a good candidate

* To whom correspondence should be addressed. E-mail: jcorbett@iastate.edu.

(1) Corbett, J. D. *Angew. Chem., Int. Ed.* **2000**, *39*, 670. Corbett, J. D. *Inorg. Chem.* **2000**, *39*, 5178. Corbett, J. D. In *Chemistry, Structure and Bonding of Zintl Phases and Ions*; Kauzlarich, S., Ed.; VCH: New York, 1996; pp 139−181. Cordier, G.; Eisenmann, B. In *Chemistry, Structure and Bonding of Zintl Phases and Ions*; Kauzlarich, S., Ed.; VCH: New York, 1996; pp 61−137.
(2) Seo, D. K.; Corbett, J. D. *J. Am. Chem. Soc.* **2000**, *122*, 9621.
(3) Häussermann, U.; Amerioun, S.; Eriksson, L.; Lee, C.-S.; Miller, G. J. *J. Am. Chem. Soc.* **2002**, *124*, 4371.
(4) Zheng, C.; Hoffmann, R. *Z. Naturforsch.* **1986**, *41B*, 292. Burdett, J. K.; Miller, G. J. *Chem. Mater.* **1990**, *2*, 12.
(5) von Fedorov, J. S. *Z. Kristallogr.* **1904**, *38*, 321.
(6) Villars, P.; Calvert, L. D. *Pearson's Handbook of Crystallographic Data for Intermetallic Phases*, 2nd ed.; American Society of Metals: Metals Park, OH, 1991.

10.1021/ic701127f CCC: $37.00
Published on Web 09/22/2007

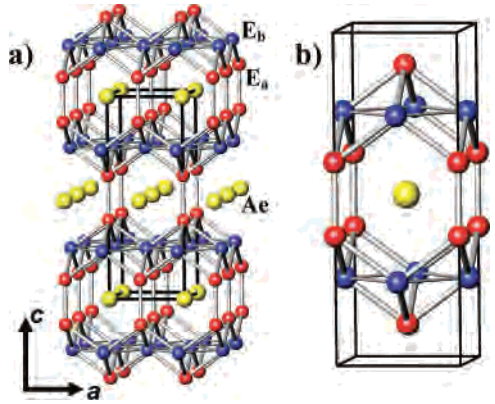

Figure 1. (a) $BaAl_4$-type structure, represented as AeE_4, features a body-centered tetragonal unit cell (space group *I*4/*mmm*, No. 139) with two independent apical E_a (red) and basal E_b sites (blue). (b) The 18-vertex Fedorov polyhedron centered by Ae.

for matrix effects because the cage dimensions are evidently closely coupled to the size of the encapsulated cation. Thus, when the cation becomes too small to match the size of the encapsulating cage, a monoclinically distorted variant of the $BaAl_4$ structure occurs, such as $CaAl_4$ and $CaGa_4$.[8] An even larger size mismatch leads to the formation of a different monoclinic structure for $EuIn_4$[9] and $SrIn_4$[2] with five-membered rather than six-membered rings.

However, the size matching necessary for the stabilization of these phases can be realized not only by means of cation alterations but also via the substitution of other elements into the polyanionic network. As shown here, the substitution of the effectively smaller Mg or Zn atoms into the indium sublattice of monoclinic $SrIn_4$ (*C*2/*m*) dramatically changes the structure into the tetragonal $BaAl_4$-type structure. A similar result has been found on mixing Au with In at the 4e sites in tetragonal $SrAuIn_3$.[10] Here, we report the syntheses and structural characterizations of a series of intermetallic compounds with $BaAl_4$-type structural features: $SrMg_xIn_{4-x}$ ($0.85 \le x \le 1.53$), $BaMg_xIn_{4-x}$ ($0 \le x \le 1.79$), $BaZn_{0.79(2)}In_{3.21}$, and $SrZn_{1.00(4)}In_{3.00}$, but a slight symmetry reduction in part of the comparable Sr−Mg−In system is observed.

Experimental Section

Syntheses. All materials were handled in N_2-filled gloveboxes with moisture levels below 1 ppm (vol). All compounds were synthesized via high-temperature reactions of the elements (99.98% magnesium, 99.999% indium, 99.9999% zinc, 99.95% strontium, and 99.9% barium, all from Alfa-Aesar). The weighed elements were enclosed in welded tantalum tubes that were in turn sealed in evacuated fused silica jackets by methods and techniques described previously.[11] Pure phases (>95%) of all reported products were synthesized directly from those compositions (judging from comparisons of their Guinier powder patterns with those calculated from the refined structures). The reaction temperature profiles were acquired by heating the samples to 1000 °C and holding there for 10 h, cooling at 10 °C/h to 600 °C, then holding there for 160 h to grow crystals followed by radiative cooling to room temperature. All compounds are silvery, brittle, and sensitive to moisture or air at room temperature.

X-ray Studies. Powder diffraction data were collected with the aid of a Huber 670 Guinier powder camera equipped with an area detector and Cu Kα radiation ($\lambda = 1.540598$ Å). Powdered samples were homogeneously dispersed between two layers of Mylar with the aid of a little vacuum grease. Single crystals were selected from the products in a glovebox and sealed in capillaries. Single-crystal diffraction data were collected at 293(2) K with Mo Kα radiation on a Bruker SMART APEX CCD diffractometer and in the form of four sets of 606 frames with 0.3° scans in ω and exposure times of 10 s per frame. The 2θ range extended from ~3° to ~57°. The unit cell parameters for each were determined from data for about 900 indexed reflections. The reflection intensities were integrated with the *SAINT* subprogram in the *SMART* software package.[12] The data were corrected for Lorentz and polarization effects, and for absorption empirically according to the program *SADABS*.[13] All structural solutions were obtained by direct methods and refined by full-matrix least-squares refinement on F_o^2 using the Bruker *SHELXTL* 6.1 software package.[14] Lattice constants for the same sample obtained by powder versus single-crystal means always agreed to within about 0.01 Å.

Electronic Structure Calculations. To better understand the chemical bonding in the structures and to gain some insight into the role of Mg in the nominal polyanionic network, tight-binding (TB) electronic structure calculations were performed on $SrMgIn_3$, the only compound reported with unmixed atoms, by both linear muffin-tin-orbital (TB−LMTO−ASA)[15] and extended Hückel TB (EHTB) methods.[16] The radii of the Wigner-Seitz (WS) spheres were assigned automatically in the former so that the overlapping potential would be the best possible approximation to the full potential.[17] No interstitial sphere was necessary with the default overlap restriction (16%). The WS radii determined by this procedure for all atoms were reasonable, 1.49 Å for In1, 1.63 Å for both In2 and Mg, and 2.34 Å for Sr.

Semiempirical EHTB band calculations allowed Mulliken atom population analyses, which provide some guidance as to charge segregation within a particular framework.[18] Mulliken populations for valence orbital occupations were evaluated by integration over a set of 216 *k* points in the irreducible wedge of the body-centered tetragonal Brillouin zone. Atomic orbital energies and exponents employed in the calculations were as follows (H_{ii} = orbital energy, eV; ξ = Slater exponent): In 5s, −12.6, 1.903; 5p, −6.19, 1.677; Mg 3s, −9.0, 1.10; 3p, −4.5, 1.10; and Sr 5s, −6.62, 1.214; 5p, −3.92, 1.214.[19]

Results and Discussion

Phase Widths of $AeMg_xIn_{4-x}$. The first single crystal in a $BaAl_4$-type structure, $SrMg_{1.532(4)}In_{2.468}$ (**I**), was obtained

(7) Wendorff, M.; Röhr, C. *Z. Anorg. Allg. Chem.* **2005**, *631*, 338.
(8) Miller, G. J.; Li, F.; Franzen, H. F. *J. Am. Chem. Soc.* **1993**, *115*, 3739. Bruzzone, G.; Fornasini, M. L.; Merlo, F. *J. Less-Common Met.* **1989**, *154*, 67.
(9) Fornasini, M. L.; Cirafici, S. *Z. Kristallogr.* **1990**, *190*, 295.
(10) Dai, J-C.; Corbett, J. D. *Inorg. Chem.* **2007**, *46*, 4592.
(11) Dong, Z-C.; Corbett, J. D. *J. Am. Chem. Soc.* **1993**, *115*, 11299.
(12) *SMART*; Bruker AXS, Inc.; Madison, WI, 1996.
(13) Blessing, R. H. *Acta Crystallogr.* **1995**, *A51*, 33.
(14) *SHELXTL*; Bruker AXS, Inc.; Madison, WI, 2000.
(15) Tank, R.; Jepsen, O.; Burckhardt, A.; Andersen, O. K. *TB−LMTO−ASA Program*, version 4.7; Max-Planck-Institut für Festkörperforschung: Stuttgart, Germany, 1994.
(16) Ren, J.; Liang, W.; Whangbo, M.-H. *CAESAR for Windows*; Prime-Color Software, Inc.; North Carolina State University: Raleigh, NC, 1998.
(17) Jepsen, O.; Andersen, O. K. *Z. Phy. B: Condens. Matter* **1995**, *97*, 35.
(18) Lee, C.-S.; Miller, G. J. *J. Am. Chem Soc.* **2000**, *122*, 4937. Lee, C.-S.; Miller, G. *Inorg. Chem.* **2001**, *40*, 338. Li, B.; Corbett, J. D. *Inorg. Chem.* **2004**, *43*, 3582.

Table 1. Summary of Reaction Compositions and Phases Identified for $AeMg_xIn_{4-x}$ (Ae = Sr, Ba) Samples Equilibrated at 600 °C[a]

loading composition	compound obtained[b]	unit cell *a*, *c* (Å)	volume (Å^3)
	$SrMg_xIn_{4-x}$[c]		
$SrMg_{1.5}In_{2.5}$	$x = 1.532(4)$	4.6814(3), 12.711(2)	278.57(4)
$SrMg_{1.25}In_{2.75}$	$x = 1.24(1)$	4.6831(3), 12.658(2)	277.61(4)
$SrMgIn_3$	$x = 1$	4.6895(7), 12.629(3)	277.7(1)
$SrMg_{0.75}In_{3.25}$	$x = 0.85(1)$	4.7093(3), 12.563(2)	278.62(4)
	$BaMg_xIn_{4-x}$		
$BaMg_2In_2$	$x = 1.788(6)$	4.8625(7), 12.515(3)	295.90(8)
$BaMg_{1.7}In_{2.3}$	$x = 1.676(8)$	4.8500(3), 12.516(2)	294.40(5)
$BaMgIn_3$	$x = 1.046(6)$	4.833(2), 12.48(1)	291.5(3)
$BaMg_{0.5}In_{3.5}$	$x = 0.52(1)$	4.8946(4), 12.268(2)	293.90(6)
$BaMg_{0.1}In_{3.9}$	$x = 0.11(1)$	4.9511(4), 12.039(2)	295.13(6)
$BaIn_4$[d]	$x = 0$	4.970(3) 11.983(3)	295.99

[a] The compositions and the unit cells were obtained from single-crystal X-ray refinements. [b] According to powder patterns, pure phases (>95%) for all compounds were obtained except for an unknown phase (<10%) with $SrMg_{0.75}In_{3.25}$ and ~15% $BaMg_{0.26}In_{1.74}$ ($CeCu_2$ type) with $BaMg_{1.788}In_{2.212}$. [c] The last three $SrMg_xIn_{4-x}$ structures crystallize in space group $I\bar{4}m2$, and all others crystallize in $I4/mmm$. [d] Reference 5b.

from a reaction with a Mg-richer composition $Sr_3Mg_{20}In_{14}$ that was designed to look for an isostructural example of $K_3Mg_{20}In_{14}$.[20] It is interesting to see that the structure obtained is of the $BaAl_4$ type instead of $SrIn_4$ type ($C2/m$), evidently because of the relative atomic size effects discussed below. As shown in Table 1, an extended search to determine the phase width of $SrMg_xIn_{4-x}$ found that two Mg-poorer compounds $SrMgIn_3$ (**II**) and $SrMg_{0.85(1)}In_{3.15}$ (**III**) crystallize with the same basic network as that for **I** but in a lower-symmetry version ($I\bar{4}m2$) in which the basal 4d site is split into independent 2c and 2d members. This space group also occurs for the higher Mg content in $SrMg_{1.24(1)}In_{2.76}$ (Table 1). This symmetry lowering to $I\bar{4}m2$ appears to be a new variant of $BaAl_4$ structure, although there are about 20 low-symmetry examples in space group $I4mm$.[6] The reason for the small symmetry change from **I** ($I4/mmm$) to **III** ($I\bar{4}m2$) may be associated with a greater stability of heteroatomic bonding between the ordered Mg and In components. Location of the transitional composition for this change is difficult. Compound **III** was obtained from a reaction with a loading composition $SrMg_{0.75}In_{3.25}$, indicating that **III** is the Mg-poorest composition at 600 °C. An unknown hexagonal phase with a possible supercell was observed from a reaction with the Mg-poorer loading composition $SrMg_{0.5}In_{3.5}$. On the other hand, reactions with Mg-richer compositions, such as $SrMg_2In_2$ and $SrMg_3In$, mainly produced $SrMg_{0.41}In_{1.59}$[21] (*Imma*, $CeCu_2$ type) and $SrMg_{4.84}In_{3.16}$[22] (*Pnma*, YCo_5P_3 type), respectively. Neither powder pattern showed any evidence of a $SrMg_xIn_{4-x}$ phase. The competitive hexagonal phase and the orthorhombic $SrMg_{0.41}In_{1.59}$ should define the observed phase width for $SrMg_xIn_{4-x}$, which is about $x = 0.85-1.53$. The formation of the orthorhombic $SrMg_{0.41}In_{1.59}$ also demonstrates a structural change from that of $SrIn_2$[23] ($CaIn_2$ type, $P6_3/mmc$) into the $CeCu_2$ type (*Imma*)

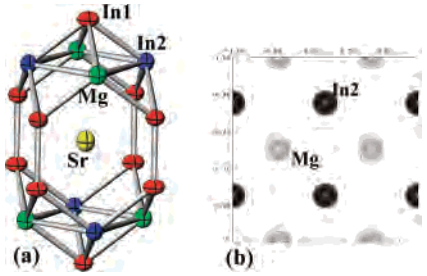

Figure 2. (a) Fedorov polyhedron centered by Sr in the well-ordered $SrMgIn_3$ structure ($I\bar{4}m2$: Sr, yellow; In1, red; In2, blue; and Mg, green). (b) Fourier synthesis map on $x,y,1/4$ plane with a contouring level of 4 e·Å^{-3}. This corresponds to the square net in a.

on the substitution of Mg atoms into the anionic sublattice.[21] A parallel structure change has also been reported in $Ba(Au,Hg)_x(In,Tl)_{2-x}$ systems.[24]

Compared with $SrMg_xIn_{4-x}$, comparable alternative phases also form in the Ba−Mg−In system from Mg-rich compositions: $BaMg_{0.26}In_{1.74}$[21] (*Imma*, $CeCu_2$ type) and $BaMg_{4.78}In_{3.22}$[22] (*Pnma*, YCo_5P_3 type) from reactions loaded as $BaMg_2In_2$ and $BaMg_3In$, respectively. No $BaMg_xIn_{4-x}$ was observed after the second reaction, but a large amount of $BaMg_xIn_{4-x}$ (≈80%) was formed after the first, and a single crystal from this was refined as $BaMg_{1.788(6)}In_{2.212}$ (**IV**) in the $BaAl_4$-type structure, indicating that it is the Mg-richest phase. As expected, lower Mg proportions show no structural change (Table 1) down to binary $BaIn_4$.[5] Thus, compared with $SrMg_xIn_{4-x}$, $BaMg_xIn_{4-x}$ exhibits a greater phase width for a $BaAl_4$-type structure, $x = 0-1.79$, inasmuch as $BaIn_4$ exists in this structure type but $SrIn_4$ does not. Neither symmetry lowering nor a well-ordered structure was observed for $BaMg_{1.046(6)}In_{2.954}$ (**V**). Attempts to synthesize well-ordered $BaZnIn_3$ and $SrZnIn_3$ also failed, rather giving $BaZn_{0.79(2)}In_{3.21}$ (**VI**) and $SrZn_{1.00(4)}In_{3.00}$ (**VII**), respectively, in $BaAl_4$-type structures. The Guinier powder patterns from the reactions leading to $BaMgIn_3$ and $SrZnIn_3$ showed only the targeted phases **V** and **VII**, respectively, and the pattern from reaction-loaded $BaZnIn_3$ presented two main phases, $BaZn_{0.8}In_{3.2}$ and $BaZn_xIn_{2x}$[21] (*Imma*, $CeCu_2$ type).

Structural Refinements. All data sets showed body-centered tetragonal lattices with no systematic absences. A noncentrosymmetric space group for **II** and **III** was indicated by their mean values of $|E^2 - 1|$ (≈ 0.69), and the structures were successfully solved in space group $I\bar{4}m2$ (No. 119). The refinement of **II** showed that the 2c and 2d sites are exclusively occupied by In and Mg, respectively (Figure 2a). (From the view of crystallography, these two sites are interchangeable.) The refinement of **III** showed that one of the two basal atom sites is mixed Mg/In, and the other is fully occupied by In. As expected, one of these two sites becomes fully occupied by Mg with more Mg substitution, and the other becomes occupied with mixed Mg/In in $SrMg_{1.24(1)}In_{2.76}$. (The crystal and refinement data are provided in Supporting Information Tables S1 and S2.) Full occupancies of mixed atom sites were assumed. Mixed Mg/In occupancies are common and have been found in interme-

(19) Canadell, E.; Eisenstein, O.; Rubio, J. *Organometallics* **1984**, *3*, 759.
(20) Li, B.; Corbett, J. D. *Inorg. Chem.* **2006**, *45*, 3861.
(21) Li, B.; Corbett, J. D., unpublished results.
(22) Li, B.; Corbett, J. D. *Inorg. Chem.* **2007**, *46*, 2237.
(23) Nuspl, G.; Polborn, K.; Evers, J.; Landrum, G. A.; Hoffmann, R. *Inorg. Chem.* **1996**, *35*, 6922.
(24) Dai, J.-C.; Corbett, J. D. *Inorg. Chem.* **2006**, *45*, 2104.

Table 2. Crystal and Refinement Data for $AeMg_xIn_{4-x}$ (Ae = Sr, Ba), $BaZn_{0.79(2)}In_{3.21}$, and $SrZn_{1.00(4)}In_{3.00}$

compound	$SrMg_{1.532(4)}In_{2.46}$ (**I**)	$SrMgIn_3$ (**II**)	$SrMg_{0.85(1)}In_{3.15}$ (**III**)	$BaMg_{1.788(6)}In_{2.212}$ (**IV**)	$BaMg_{1.046(6)}In_{2.954}$ (**V**)	$BaZn_{0.79(2)}In_{3.21}$ (**VI**)	$SrZn_{1.00(4)}In_{3.00}$ (**VII**)
fw	407.97	456.39	470.42	434.66	502.04	557.80	497.45
space group, *Z*	*I*4/*mmm*, 2	$I\bar{4}m2$, 2	$I\bar{4}m2$, 2	*I*4/*mmm*, 2	*I*4/*mmm*, 2	*I*4/*mmm*, 2	*I*4/*mmm*, 2
a (Å)	4.6814(3)	4.6895(7)	4.7093(3)	4.8625(7)	4.833(2)	4.7827(8)	4.627(1)
c (Å)	12.711(2)	12.629(3)	12.563(2)	12.515(3)	12.48(1)	12.007(4)	12.098(5)
V (Å^3)	278.57(4)	277.7(1)	278.62(4)	295.90(8)	291.5(3)	274.7(2)	259.0(1)
ρ_{calc} (g/cm^3)	4.86	5.46	5.61	4.88	5.72	6.75	6.38
μ (Mo Kα, mm^{-1})	19.6	21.8	21.2	15.1	18.2	23.6	27.8
R1/wR2, $I > 2\sigma(I)$	0.013/0.030	0.015/0.031	0.023/0.055	0.013/0.029	0.015/ 0.035	0.015/ 0.034	0.023/ 0.065
R1/wR2, all data	0.013/0.030	0.015/0.031	0.023/0.055	0.014/0.029	0.015/0.035	0.016/0.035	0.023/0.065
largest diff peak and hole (e·Å^{-3})	0.54, −1.12	0.42, −0.85	0.58, −1.26	0.60, −0.59	0.66, −0.97	0.77, −0.78	0.82, −1.49

tallic compounds such as $K_{34}Mg_{13.78}In_{91.22}$,[25] $Rb_{14}(Mg_{1-x}In_x)_{30}$,[26] $AeMg_5In_3$,[22] and $Ir_3Mg_{17.1(1)}In_{1.9(1)}$.[27] Refinements of both **II** and **III**, finally with anisotropic displacement parameters and secondary extinction corrections, converged very well, such as R1 = 0.015, wR2 = 0.031 ($I > 2\sigma(I)$), and the largest peak of 0.42 e/Å^3 for **II**. Attempts to solve these structures in high-symmetry space group I4/*mmm* failed, with final refinements converging at very high *R* values and with very large residual peaks. For example, the final refinement for **II** converged at R1 = 0.142, wR2 = 0.3513 ($I > 2\sigma(I)$), and with a peak of 12.7 e/Å^3 at the basal atom site. Evidence of lower symmetry was also shown in the Fourier synthesis map (Figure 2b). Two totally different electron densities at the four basal atom sites indicate the disappearance of the proper 4-fold axis of the $BaAl_4$ structure. Different electron densities at the basal atom sites were also observed in two other compounds with a lower symmetry, **III** and $SrMg_{1.24(1)}In_{2.76}$ (Figure S1b, Supporting Information).

A centrosymmetric space group for **I** was indicated by the intensity statistics $|E^2 - 1| \approx 0.89$, and the structure was easily solved as a $BaAl_4$-type structure (*I*4/*mmm*) with mixing of In/Mg (0.234(2)/0.766) on the basal site (4d). An attempted refinement in space group $I\bar{4}m2$ gave higher *R* values. Moreover, a refinement in the lower space group showed the same mixing at the 2c and 2d sites: 0.24(1)In/0.76Mg and 0.23(2)In/0.77Mg, respectively, both of which now have much higher errors in the occupancy deviations. Similar peak heights were found at the four basal atom sites in Fourier maps synthesized in the low-symmetry space group (Figure S2, Supporting Information). Different electron densities at these sites would be expected if the structure did not have a proper 4-fold axis through the center of the square net. The structures of **IV**−**VII** were similarly solved on the bases of the $BaAl_4$ model. The refinements showed mixed 0.106(3)In/0.894Mg and 0.477(2)In/0.523Mg atoms at the basal sites (4d) in **IV** and **V**, respectively, but mixed In/Zn atoms with occupancies of 0.607(9)/0.393 and 0.50(2)/0.50 at the apical atom sites (4e) in **VI** and **VII**, respectively. The different site preferences between Mg and Zn are related to their different atomic sizes and electronegativities, as discussed below.

The crystallographic and refinement parameters for all compounds are given in Table 2. Table 3 gives the corresponding atomic positional and isotropic-equivalent displacement parameters and occupancies. Table 4 contains selected interatom distances for these compounds. More detailed crystallographic and refinement data and the anisotropic displacement parameters are available in the Supporting Information (CIF).

Table 3. Atomic Coordinates (all with $x = 0$), Isotropic-Equivalent Displacement Parameters (Å^2 x 10^3), and Site Occupancies for **I**−**VII**[a]

atom	site	y	z	*U*(eq)	occupancy (In/M)
			$SrMg_{1.532(4)}In_{2.468}$ (**I**)		
Sr	2a	0	0	17(1)	1.00
In1	4e[b]	0	0.6105(1)	16(1)	1.00
In2/Mg	4d[c]	1/2	1/4	17(1)	0.234/0.766(2)
			$SrMgIn_3$ (**II**)		
Sr	2a	0	0	17(1)	1.00
In1	4e	0	0.6108(1)	16(1)	1.00
In2	2c	1/2	1/4	16(1)	1.00
Mg	2d	1/2	3/4	14(1)	1.00
			$SrMg_{0.85(1)}In_{3.15}$ (**III**)		
Sr	2a	0	0	18(1)	1.00
In1	4e	0	0.6111(1)	18(1)	1.00
In2	2c	1/2	1/4	18(1)	1.00
In/Mg	2d	1/2	3/4	18(1)	0.15/0.85(1)
			$BaMg_{1.788(6)}In_{2.212}$ (**IV**)		
Ba	2a	0	0	16(1)	1.00
In1	4e	0	0.6143(1)	17(1)	1.00
In2/Mg	4d	1/2	1/4	18(1)	0.106/0.894(3)
			$BaMg_{1.046(6)}In_{2.954}$ (**V**)		
Ba	2a	0	0	16(1)	1.00
In1	4e	0	0.6140(1)	17(1)	1.00
In2/Mg	4d	1/2	1/4	18(1)	0.477/0.523(2)
			$BaZn_{0.79(2)}In_{3.21}$ (**VI**)		
Ba	2a	0	0	15(1)	1.00
In1/Zn	4e	0	0.6118(1)	19(1)	0.607/0.393(9)
In2	4d	1/2	1/4	21(1)	1.00
			$SrZn_{1.00(4)}In_{3.00}$ (**VII**)		
Sr	2a	0	0	16(1)	1.00
In1/Zn	4e	0	0.6072(1)	17(1)	0.50/0.50(2)
In2	4d	1/2	1/4	18(1)	1.00

[a] Compounds **II** and **III** crystallize in $I\bar{4}m2$, and all others crystallize in *I*4/*mmm*. [b] Apical site. [c] Basal site.

Size Effects. In the $BaAl_4$-type structure, the size match between electropositive Ae and the encapsulating cage represents an evidently important feature of structural stability.[3] In both $AeMg_xIn_{4-x}$ systems, the unit cells along the *a* and *b* axes decrease with increasing Mg substitution (Table 1) consistent with the relatively smaller radius of Mg versus In (1.38 vs 1.44 Å in Pauling single-bond metallic radii).[28] At the same time, the unit cells increase along the *c* axis to

(25) Li, B.; Corbett, J. D. *Inorg. Chem.* **2006**, *45*, 8958.
(26) Li, B.; Corbett, J. D. *Inorg. Chem.* **2006**, *45*, 156.
(27) Hlukhyy, V.; Pöttgen, R. *J. Solid State Chem.* **2005**, *178*, 79.
(28) Pauling, L. *Nature of the Chemical Bond*, 3rd ed.; Cornell University Press: Ithaca, NY, 1960; p 403.

Table 4. Selected Bond Lengths (Å) for **I**−**VII**: Ae = Sr or Ba. E_a is Apical Site 4e (0,0,*z*), and E_b is Basal Site 4d ($0,^1/_2,^1/_4$)

compound	Ae−E_a	Ae−E_b	E_a−E_b	E_b−E_b	E_a−E_a
$SrMg_{1.532(4)}In_{2.468}$ (**I**)	3.5957(2)	3.9468(3)	2.9369(3)	3.3102(2)	2.8080(8)
$SrMgIn_3$ (**II**)	3.5991(5)	3.9327(7)	2.9306(4)	3.3160(5)	2.799(1)
$SrMg_{0.85(1)}In_{3.15}$ (**III**)	3.6105(4)	3.9254(3)	2.9311(6)	3.3300(2)	2.791(2)
$BaMg_{1.788(6)}In_{2.212}$ (**IV**)	3.7242(5)	3.9623(5)	2.9654(4)	3.4383(5)	2.8619(9)
$BaMg_{1.046(6)}In_{2.954}$ (**V**)	3.702(1)	3.946(2)	2.953(1)	3.418(1)	2.845(2)
$BaZn_{0.79(2)}In_{3.21}$ (**VI**)	3.6387(6)	3.8378(8)	2.9104(6)	3.3819(7)	2.686(2)
$SrZn_{1.00(4)}In_{3.00}$ (VII)	3.5195(9)	3.808(2)	2.887(1)	3.2718(7)	2.594(4)

minimize the packing change (Figure 1b). Such contradictory changes result in interesting unit cell volume changes in both $AeMg_xIn_{4-x}$ systems. As before,[3] the volume of the cage may be simply defined as the volume of the Fedorov polyhedron (Figure 1b), which corresponds to one-half of the unit cell volume. This volume decreases with decreasing Mg in $SrMg_xIn_{4-x}$ over $x = 1.53$ (**I**) to 1.24, then increases at $x = 0.85$ (**III**). Both the Mg-richest (**I**) and Mg-poorest (**III**) phases have a very similar cage volume (139.3 Å^3), which probably is the upper limit of the size for such an encapsulating cage centered by Sr. Besides the existence of the competitive phases as mentioned above, this upper limit may be another reason for the phase width of $SrMg_xIn_{4-x}$. This upper limit also can explain the nonexistence of tetragonal structure, inasmuch as such a $SrIn_4$ would have a cage size of 149.1 Å^3,[29] too large for matching Sr. Amazingly, this observed volume maximum is also very close to that for each Sr in monoclinic $SrIn_4$ (139.5 Å^3).[2] Similar packing efficiency is shown in both monoclinic and tetragonal structures.

An unusual volume change was also observed in the $BaMg_xIn_{4-x}$ system: from 295.99 Å^3 for $BaIn_4$[5] decreasing to 291.5(3) Å^3 for $x = 1.0$ (**V**), then increasing to 295.90(8) Å^3 at $x = 1.79$ (**IV**). Notice that both the Mg-richest (**IV**) and Mg-free ($BaIn_4$) phases reach the same cage volume (148.0 Å^3). However, a larger cage volume might still be reachable for Ba with a larger anion, as found for $BaTl_{0.63}In_{3.37}$,[30] the Tl-richest phase with $BaAl_4$-type structure with a cage volume of 149.9 Å^3. Further increases in Tl proportions would cause the size mismatching found in $BaTl_4$, which has a monoclinic $SrIn_4$-type structure.[31] The difference of the observed maximal cage volumes for Ba and Sr in Ae−Mg−In systems, about 8.7 Å^3, matches almost perfectly the volume increment established by Biltz[32] ($V(Sr^{2+}) = 18.3$ Å^3, $V(Ba^{2+}) = 26.6$ Å^3, $\Delta = 8.3$ Å^3. Such constant volume changes as a function of Ae were also reported in $AeZn_{2-\delta}M_{2-\delta}$ (Ae = Ca, Sr, Ba; M = Al, Ga) systems, in which only the upper limit for Ca was achieved.[3] The smaller anions, such as Al and Ga, would not allow testing the upper limit volumes with Sr or Ba.

In contrast to the substitution of In by Mg, that by the smaller Zn (1.31 Å)[28] leads to a considerably greater shrinkages of the unit cell volumes (Table 2) as well as of some bond distances (Table 4). A number of the distance changes in these compounds are noteworthy. Compared with the Ae−E_a distances, all Ae−E_b distances are quite long, but the latter still show a small bonding character at E_F and positive integrated crystal overlap Hamiltonian populations (−ICOHP) values in **II** (below). All E_b−E_b distances in the basal plane are similar and not particularly unusual, being 0.4−0.5 Å greater than $d(E_a-E_b)$, and even greater than $d(E_a-E_a)$. These basal plane interactions, which have generally been concluded to be nonbonding in two extensive analyses of $BaAl_4$-type compounds,[4] show antibonding character at E_F but non-negligible −ICOHP values (below). The ranges of the E_a−E_a distances are quite large among different systems, readily adapting to the size of Ae, whereas the E_a−E_b distances have a rather small range. The greater flexibility of the E_a−E_a interactions, basically only with a variation in *c*, allows the substitution of the much smaller Zn atom there. A substitution of Zn in the basal atom sites would make the E_b−E_b distances too short, which can explain the Zn site preference in **VI** and **VII**.

Site Preferences. The structures of all compounds studied display clear site preferences between magnesium and zinc: all magnesium atoms occupy basal atom sites (E_a) and all zinc atoms occupy apical sites (E_b, 4d). The same basal site preference for Mg also occurs in other $BaAl_4$ family compounds such as $AeMg_{1.7(1)}Ga_{2.3}$ (Ae = Ba, Sr),[3] $BaMg_2Si_2$,[33] $BaMg_2Ge_2$,[33] and $EuMg_{0.56}Ga_{3.44}$[34] according to X-ray refinements and in $SrMg_{0.9}Al_{3.1}$ and $BaMg_{0.9}Al_{3.1}$ according to energies of different coloring schemes obtained from ab initio calculations.[3] Previous theoretical studies based on Mulliken overlap population analyses obtained from semiempirical TB calculations suggested that the element with greater electronegativity is better bound in the apical site.[4] For example, Au with greater electronegativity occupies the apical site in $BaAuIn_3$, $BaAuTl_3$, and $SrAuIn_3$ ($BaAl_4$ type).[35,10] The Mg site preference at the basal atom site shown in all of the present compounds is also consistent with its smaller electronegativity on the Pauling scale relative to those of another post-transition elements.[36] (The order of course does not agree with the fundamentally different Mulliken scale.)

However, zinc site preferences in $BaAl_4$-type structures seem more complicated, and different site preferences have been reported. Zinc has also been found at basal sites in $AeZn_2Ge_2$ (Ae = Ca, Eu),[37] $AeZn_2Si_2$ (Ae = Ca, Eu),[37,38] and $SrZn_2Ge_2$,[39] in which the electronegativity of Zn on the

(29) Amerioun, S.; Häussermann, U. *Inorg. Chem.* **2003**, *42*, 7782.
(30) Palasyuk, A.; Corbett, J. D. *Z. Anorg. Allg. Chem*, accepted.
(31) Dai, J-C; Corbett, J. D., unpublished results.
(32) Biltz, W. *Raumchemie der festen Stoffe*; Verlag Leopold Voss: Leipzig, 1934.
(33) Eisenmann, B.; May, N.; Müller, W.; Schäfer, H.; Weiss, A.; Winter, J.; Ziegleder, G. *Z. Anorg. Allg. Chem.* **1974**, *403*, 163.
(34) Fedorchuk, A.; Prots, Yu.; Grin, Yu. *Z. Kristallogr.* **2005**, *220*, 317.
(35) Liu, S.; Corbett, J. D. *Inorg. Chem.* **2004**, *43*, 4898.
(36) Pauling, L. *J. Am. Chem. Soc.* **1932**, *54*, 3570. Pauling's electronegativities for In, Mg, and Zn are 1.78, 1.31, and 1.65, respectively.

Table 5. Relative Total Energies (eV/f.u.) Calculated for Two Models of $AeMIn_3$ by TB−LMTO−ASA Methods[a]

model	$SrMgIn_3$	$BaMgIn_3$	$BaZnIn_3$	$SrZnIn_3$
M, basal (4d)	0	0	0.151	0.367
M, apical (4e)	0.180	0.079	0	0

[a] All energies are relative to the lowest energy arrangement for each composition.

Pauling scale is smaller than that of the respective p element, consistent with the Zn site preference. (However, in $YbZnGa_3$[40] the Zn presence on the apical site appears to have been assumed.) But when the electronegativity difference is very low, different site preferences might be expected, as shown in many Zn-containing systems. For example, with similar Pauling electronegativities for Zn (1.65) and Al (1.61), the site preference is also influenced by the size of the cation component.[3] Zinc occurs on apical sites in $REZn_2Al_2$ (RE = La, Ce)[41] and $REZn_{1.66}Al_{2.34}$ (RE = Yb, Nd),[42] but mixed Zn/Al occupancies are found in both sites in $AeZn_{\sim 2}Al_{\sim 2}$ (Ae = Ca, Sr, Ba).[3] In the present cases, Zn takes the apical site in both **VI** and **VII** even though its electronegativity is smaller than that of In. The site preference problem in the ternary $BaAl_4$-type structure appears to be more than just an issue relating to electronegativity differences. With the large size difference between Zn and In, the site preference may be more related to the size match, as mentioned above, rather than their electronegativity difference. The interplay of size and electronic factors makes the atomic site preference more complex.

In order to understand the observed site preferences better, the total energies were calculated by a TB−LMTO−ASA approach for different atom arrangements, a method that has been successful in explaining coloring problems in many compounds,[43] including some $BaAl_4$-type structures.[3] On the other hand, the calculated total energies from ab initio calculations for different schemes do not necessarily correlate with the differences in electronegativities. Here, we explored the total electronic energy differences for $AeMIn_3$ (Ae = Ba, Sr; M = Mg, Zn) in two different atom arrangements for M and In atoms: (i) M in two of the four basal sites, (ii) M in two of the four apical sites, and In in the other sites. The reported unit cells and atomic positions were used for the static structure calculations, and different space groups $I\bar{4}m2$(No. 119) and $I4mm$ (No. 107) were employed for i and ii, respectively, in order to have ordered distributions. Such symmetry changes do not make a difference in terms of total energy. The results are summarized in Table 5 relative to the lowest energy arrangement for each composition. The results show that Mg and Zn atoms prefer the basal sites (4d) and the apical sites (4e), respectively, consistent with the experimental results.

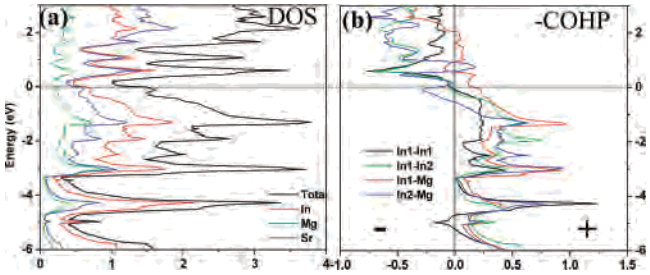

Figure 3. TB−LMTO−ASA electronic structure calculation results for $SrMgIn_3$. (a) Total DOS (black) and partial DOS curves: In (red), Mg (green), and Sr (blue). (b) −COHP data for In1−In1 (black), In1−In2 (green), In1−Mg (red), and In2−Mg (blue). The dotted line denotes the Fermi level.

Electronic Structure and Chemical Bonding. LMTO results for $SrMgIn_3$ (**II**) will be used to rationalize the chemical bonding. As shown in the density of states (DOS) in Figure 3a, the Fermi level intersects a finite DOS, and the minimum DOS at the nearby pseudogap corresponds to 13.15 valence electrons, 0.15 valence electrons per formula unit above that in **II**, which may reflect some additional site preference energies for the electron-poorer Mg. The DOS contributions of Sr, Mg, and In orbitals at E_F are about 38, 17, and 45%, respectively. Taking into account the number of each atom in the formula, Sr makes the largest contribution, mainly from the d orbitals (Figure S3, Supporting Information), and that from Mg is particularly small. Similarly large contributions from Sr were also found in $SrIn_4$ and Sr_3In_{11} structures studied by a LMTO−ASA method.[29] The contribution of the Sr states is rather low below the Fermi level and increases above. This behavior is typical for polar intermetallic compounds and Zintl phases, which formally are composed of an oxidized electropositive component (the active metal) and a polyanionic (reduced) network. To check the interactions between atom types, the integrated crystal orbital Hamilton population analyses (−COHP) were also evaluated (Figure 3b). At the Fermi level, both In1−In1 and In1−In2 are effectively optimized, whereas substantial bonding and antibonding characters are shown for In1−Mg (2.931 Å) and In2−Mg (3.316 Å), respectively, which are reasonable according to their distances. To quantify the interaction between atoms, the integrated −ICOHP values were also determined. The values for In1−In1 (2.799 Å) and In1−In2 (2.931 Å) are quite large, 2.00 and 1.63 eV/bond, respectively. The long interaction of In2−Mg in the basal plane has a much smaller but non-negligible value (0.69 ev/bond). However, the −ICOHP value for In1−Mg (E_a-E_b) is fairly large too, 1.37 eV/bond, indicating very substantial In−Mg bonding interactions, from which small positive charges for Mg might be expected. The −ICOHP values for In−Sr and Mg−Sr are about 0.42 and 0.33 eV/bond, respectively, similar to that for In−Sr in $SrMg_5In_3$.[22]

(37) Eisenmann, B.; May, N.; Müller, W.; Schäfer, H.; Weiss, A.; Winter, J.; Ziegleder, G. *Z. Naturforsch., B* **1970**, *25*, 1350. Kranenberg, C.; Johrendt, D.; Mewis, A.; Pöttgen, R.; Kotzyba, G.; Trill, H.; Mosel, B. D. *J. Solid State Chem.* **2002**, *167*, 107.
(38) Grystiv, A.; Kaczorowski, D.; Leithe-Jasper, A.; Rogl, P.; Godart, C.; Potel, M.; Noël, H. *J. Solid State Chem.* **2002**, *163*, 37.
(39) Dörrscheidt, W.; Niess, N.; Schäfer, H. *Z. Naturforsch.* **1976**, *31B*, 890.
(40) Grin, Yu.; Hiebl, K.; Rogl, P. *J. Alloys Compd.* **1995**, *227*, L4.
(41) Ikromov, A. Z.; Ganiev, I. N.; Kinjibalo, V. V. *Dokl. Akad. Nauk Tadzh. SSR* **1990**, *33* (3), 173. Cordier, G.; Czech, E.; Schäfer, H.; Woll, P. *J. Less-Common Met.* **1985**, *110*, 327.
(42) Stel'makhovych, B.; Stel'makhovych, O.; Kuz'ma, Yu. *J. Alloys Compd.* **2005**, *397*, 115.
(43) Miller, G. *Eur. J. Inorg. Chem.* **1998**, 523. Misra, S.; Miller, G. *J. Solid State Chem.* **2006**, *179*, 2290.

The Mulliken site population analyses for $SrMgIn_3$ from EHTB calculations show that the estimated charges of Sr, Mg, and In are around +1.49, +0.28, and −0.59, respectively. The value for Mg is similar to those for Mg in $K_3Mg_{20}In_{14}$[20] and $AeMg_5In_3$ (Ae = Ba, Sr),[22] which have dominant Mg−In bonding. At the same time, the value is notably smaller than those so estimated[20] for Mg in Mg_2Zn_{11} (+1.49)[44] and $Mg_2Cu_6Ga_5$ (+1.48)[45] in which Mg is the best electron donor and appears to act more as a spacer. Even allowing for the limitations of these Mulliken analyses, the results clearly show that Mg atoms show an important participation in the covalent bonding of the present structures. The well-differentiated roles of Mg in the last two compounds and others are obvious.

Conclusion

The $BaAl_4$−type structure is widely adopted among intermetallic compounds, but $SrIn_4$ crystallizes in a totally different monoclinic structure because of the size mismatch between Sr and In. However, size matching and stabilization of these phases can be realized by the substitution of other elements, such as Mg or Zn, into the nominal indium polyanionic network in AeM_xIn_{4-x} (Ae = Sr, Ba; M = Mg, Zn) systems. These compounds display the effects of anion sizes on the structural stability as well as different site preferences between Mg and Zn. With a large anion in the polyanionic network, the AeM_xIn_{4-x} systems offer the possibility of determining the upper limit volume of the encapsulating cage in order to match the size of Ae.

Acknowledgment. This research was supported by the Office of the Basic Energy Sciences, Materials Sciences Division, U.S. Department of Energy (DOE) and performed in the Ames Laboratory, which is operated for DOE by Iowa State University under Contract No. DE-AC02-07Ch11358.

Supporting Information Available: Refinement parameters for compounds **I**−**VII** in CIF format, crystal and refinement data for $SrMg_{1.24(1)}In_{2.76}$, Fourier synthesis maps of $SrMg_{1.24(1)}In_{2.76}$ and **I** with the corresponding structure pictures, and partial DOS curves for different Sr orbitals. This material is available free of charge via the Internet at http://pubs.acs.org.

IC701127F

(44) Samson, S. *Acta Chem. Scand.* **1949**, *3*, 835.
(45) Lin, Q.; Corbett, J. D. *Inorg. Chem.* **2003**, *42*, 8762. Samson, S. *Acta Chem. Scand*. **1949**, *3*, 809.